



Article

# Flow Hydrodynamics across Open Channel Flows with Riparian Zones: Implications for Riverbank Stability

Da Liu <sup>1</sup>, Manousos Valyrakis <sup>1,\*</sup>  and Richard Williams <sup>2</sup> 

<sup>1</sup> Infrastructure and Environment Research Division, School of Engineering, University of Glasgow, Glasgow G12 8QQ, UK; d.liu.2@research.gla.ac.uk

<sup>2</sup> School of Geographical and Earth Sciences, University of Glasgow, Glasgow G12 8QQ, UK; richard.williams@glasgow.ac.uk

\* Correspondence: manousos.valyrakis@glasgow.ac.uk; Tel.: +44-(0)-141-330-5209

Received: 12 June 2017; Accepted: 12 September 2017; Published: 20 September 2017

**Abstract:** Riverbank vegetation is of high importance both for preserving the form (morphology) and function (ecology) of natural river systems. Revegetation of riverbanks is commonly used as a means of stream rehabilitation and management of bank instability and erosion. In this experimental study, the effect of different riverbank vegetation densities on flow hydrodynamics across the channel, including the riparian zone, are reported and discussed. The configuration of vegetation elements follows either linear or staggered arrangements as vegetation density is progressively increased, within a representative range of vegetation densities found in nature. Hydrodynamic measurements including mean streamwise velocity and turbulent intensity flow profiles are recorded via acoustic Doppler velocimetry (ADV)—both at the main channel and within the riverbank. These results show that for the main channel and the toe of riverbank, turbulence intensity for the low densities ( $\lambda \approx 0$  to  $0.12 \text{ m}^{-1}$ ) can increase up to 40% compared the case of high densities ( $\lambda = 0.94$  to  $1.9 \text{ m}^{-1}$ ). Further analysis of these data allowed the estimation of bed-shear stresses, demonstrating 86% and 71% increase at the main channel and near the toe region, for increasing densities ( $\lambda = 0$  to  $1.9 \text{ m}^{-1}$ ). Quantifying these hydrodynamic effects is important for assessing the contribution of physically representative ranges of riparian vegetation densities on hydrogeomorphologic feedback.

**Keywords:** riverbank hydrodynamics; velocity profile; riparian zone; turbulence; open-channel flow; streambank erosion; hydrogeomorphologic feedbacks

## 1. Introduction

More than six decades of research on the influence of riparian and aquatic vegetation on fluvial systems has demonstrated that both an important and complex interdependence in terms of river hydrodynamics, sediment transport and morphology exists [1]. This has a wide range of implications, such as managing hydraulic roughness for flood control, and maintaining stream bed and bank stability during extreme hydrologic events to prevent damage to property and critical infrastructure. In particular, riverbank erosion is a significant topic for fluvial geomorphology, engineering ecohydraulics and river management because it can cause loss of land, increase sediment flux to a river and subsequently reduce channel conveyance (see for example collapsed riverbank, more than 2 m high, in Figure 1a). Revegetation of streambanks is commonly used as a best practice for restoring riparian corridors and managing streambank erosion, according to leading environment protection agencies in the UK and USA (Figure 1b) [2–4]. Practice guidance emphasizes the need to predict and quantify how riparian vegetation may affect flow hydrodynamics, influencing riverbank erosion. Guidance also notes that a degree of bank erosion is natural and the emergence of gaps in

vegetation cover, often caused by tree collapse, is essential for the natural renewal of bank vegetation. Indeed, natural river systems are highly complex due to their irregular geometry, unsteady flow and, different vegetation types and spatial patterns.

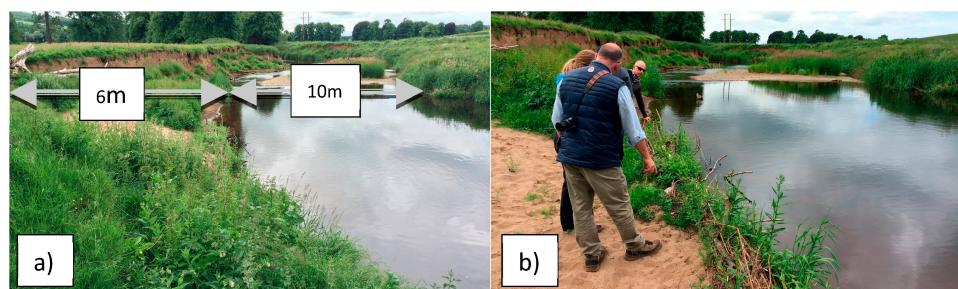


**Figure 1.** (a) Demonstration of successful riverbank stabilization efforts via revegetation of a streambank and (b) a visibly failed riverbank at a tributary of the Water of Girvan, Scotland. Bank-erosion protection work has been undertaken along this river by engineers and scientists of the Ayrshire River Trust (ART) using native plants and willow fagots to redirect the flow towards the main channel. Notice the height of the collapsed streambank (>2 m) relative to the size of ART's engineers.

An increasing number of experimental studies on vegetation hydrodynamics have been carried out over the last three decades. For example, Zong and Nepf [5] conducted a series of flume experiments to assess the effect of a staggered array of circular cylinders on flow hydrodynamics. Their results clearly show that flow velocities are affected at both the nonvegetated region and the edge of the vegetation patch. A series of visualization experiments conducted by Valyrakis et al. [6], confirm that turbulence and large-scale vortices were generated at a certain distance after the vegetation elements. Similar studies have shown that a direct link exists between the size of eddies shed downstream from vegetation elements and their capacity to scour the bed surface [7].

Bed sediment rates and bed-load flux predictions are related to the vegetation type and patch location, bed grain size and sediment supply, but the effect of individual vegetation elements may be sometimes ignored [8]. In studies to investigate the influence of vegetation patch configuration on hydrodynamics and bed load transport, vegetation density can be adjusted in many ways, such as changing the vegetation type and increasing the number of the elements in the same region. For instance, Wilson et al. [9] studied arrays of submerged flexible vegetation in rivers, and they adjusted the vegetation density by adding fronds on the same array of rods. The addition of vegetation on a sand bar induced changes in the hydrodynamic field in and around that geomorphic feature, leading to scouring at its interface with the main channel (as reported from a field study in [10]).

Riverbank vegetation is an important component of riparian vegetation affecting erosional or depositional patterns, thus its morphological and by extension ecological features. It can be seen from a few studies that riparian vegetation can drastically reduce the mean velocity at the riverbank, while increasing it at the main channel. Enhanced momentum and energy transfer take place at the bottom of the interface of the vegetated riverbank and the main channel [11]. Further, the slope of riverbanks can be another parameter affecting bank stability. Steeper riverbanks can cause greater Reynolds stresses on the bank surface. However, bank slope may not influence the lateral momentum change [12]. Near-bed turbulence and Reynolds stresses may increase at the main channel, particularly at the bottom of the boundary region between the main channel and the riverbank, with increased riverbank vegetation density [12]. However, increasing bank stability may at the same time increase the potential for erosion at the main channel, having adverse effects. Riverbank vegetation may increase the mean streamwise velocity at a small distance away from the vegetated riverbank, resulting in characteristic S-shaped mean velocity profiles [13]. For a given discharge, the flow depth at section of a vegetated stream can be affected by the increased hydraulic roughness due to the riverbank vegetation, although this also depends on the exact features of the vegetation [14].

Riverbank erosion generally involves one of the following mechanisms or a combination of some of them: mass failure, hydraulic erosion and subaerial erosion [15,16]. Subaerial erosion involves changes in soil moisture, which effectively weakens the streambank leading to the collapse of slabs of soil [15,17]. Hydraulic erosion, including sediment transport due to turbulent flows, may be more pronounced following subaerial erosion [16]. In addition, hydraulic erosion at the toe region of the riverbank can decrease the stability of the bank, causing mass failures [18]. Many previous studies show that riparian vegetation can prevent bank failure due to root reinforcement of the soil [19]. This can also be beneficial for fluvial ecosystems [20]. Chen et al. [21] conducted a set of flume experiments, with submerged instream vegetation of different densities, to assess the change in flow hydrodynamics, including velocity and turbulence, and the impact on local scouring around vegetation elements. A series of controlled flume experiments at the St Anthony Falls Laboratory (SAFL) outdoor stream facility, identified that plants' morphological characteristics, such as plant height and patch density, affect their probability of burial or uprooting and are important for their survival [22]. A numerical model developed by Schmeeckle [23] illustrates the significance of flow turbulence on sediment transport. Other numerical prediction and statistical models ([24,25] respectively) outline the importance of turbulent energetic flow structures, for promoting sediment transport processes.

Even though our understanding of the processes of bank stability has improved over the last decade, there still exists a knowledge gap on the impacts of riparian vegetation on streambank erosion [26]. Although vegetation hydrodynamics have been researched intensively, the ways by which riparian vegetation affects hydrodynamics both within the riverbank and the main channel, have not been investigated with a focus on streambank stability. To understand and comprehensively quantify how riparian vegetation affects bank stability, well controlled flume experiments covering a wide range of simulated riverbank vegetation densities, specifically designed to represent natural systems and associated hydrodynamics, are presented herein. Instantaneous three-dimensional velocity measurements are obtained using acoustic Doppler velocimetry (ADV) over a dense measurement grid across the whole channel. Analysis of the flow hydrodynamics, including mean velocity and turbulence intensity profiles across the whole channel cross section is presented, for a range of vegetation densities, and linear or staggered arrangements of the individual elements.

These results are further discussed in the context of bank erosion and implications for river management by means of re-vegetating streambanks. It is found that, both the mean and fluctuating velocity levels in the vegetated riverbank are reduced with increasing vegetation density. However, this is not the case for the main channel, up to the region near the toe of the riverbank. Specifically it is observed that the turbulence intensity near the bed surface for the low riverbank vegetation densities ( $\lambda \approx 0$  to  $0.12 \text{ m}^{-1}$ ) can increase up to 40% compared the case of high riverbank vegetation densities ( $\lambda = 0.94$  to  $1.9 \text{ m}^{-1}$ ). In addition to the above analysis, the bed-shear stresses are estimated to significantly increase at the main channel with the riverbank vegetation densities.

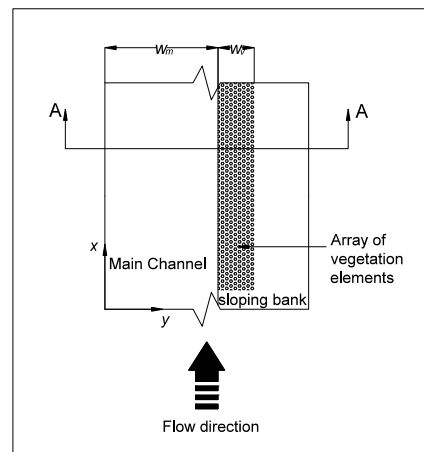
The major findings of this paper is summarized as follows:

- Flow hydrodynamics were measured across an open channel with a riverbank, for a range of riverbank vegetation densities, representative of natural systems.
- At the main channel, bed-shear stresses increase nearly twofold with a change from no vegetation to the dense vegetation ( $\lambda = 1.9 \text{ m}^{-1}$ ).
- Near the riverbank toe, turbulence intensity reduces up to 40% for the cases of low to high vegetation densities ( $\lambda \approx 0$  to  $1.9 \text{ m}^{-1}$ ).
- Recommendations are offered for improving the existing practices deploying riverbank revegetation as an environmentally sustainable method against riverbank destabilization.

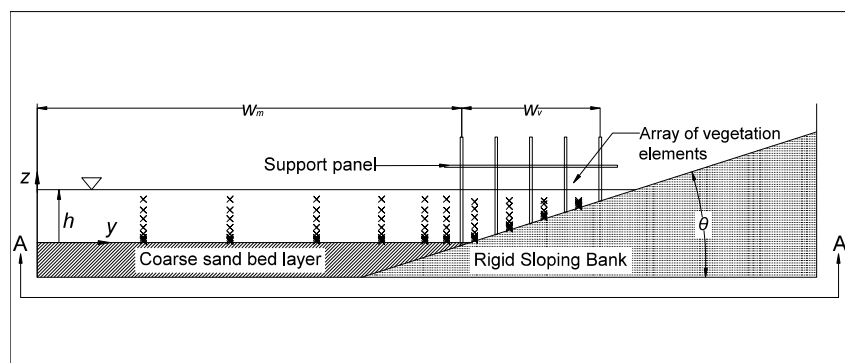
## 2. Materials and Methods

A series of flume experiments were conducted at a 14 m long by 1.8 m wide glass-walled recirculating horizontal flume, at the Water Engineering Laboratory of the University of Glasgow. The streambank was modeled by a 0.8 m wide, inclined acrylic panel with an angle,  $\theta = 17^\circ$ , running a

streamwise length of  $L = 8$  m, a short distance downstream of the inlet section of the flume (Figure 2). Flow in and out of the modified channel geometry with the riverbank cross-section was smoothly streamlined using airfoil-wing shaped sections. From the beginning of the inclined riverbank and for 8 m, the main channel section (of width  $W_m = 1$  m) was layered with coarse sand of nominal diameter ranging from 1.4–2.35 mm, with  $D_{50} = 2$  mm, up to a height of 7.5 mm (Figure 2b). A filter layer of cobbles with 20–30 mm nominal diameter starting at 2 m downstream of the inlet section and running about 1.5 m long was designed to prevent loss of the bed material from the main channel, when the flume was drained. In addition, another similar filter layer was designed before the outlet section.



(a)



(b)

**Figure 2.** (a) Plan view of a subsection of the channel setup; (b) Cross-sectional layout of the channel setup with vegetation, simulated by an array of vegetation elements (rods) placed at a variable density along the floodplain. The acoustic Doppler velocimetry (ADV) measurement grid locations are shown with the symbols (x). A-A indicates the cross section along which measurements take place.

Flow uniformity was established by appropriately adjusting the flume's tailgate height through a gear system. The flow rate controlled via two pump inverters remains fixed at all runs, as was also validated by the indications of the electromagnetic flow meters. The flow conditions were chosen appropriately and remain fixed, so that the bed surface remains unchanged during the experiments, as measured with the aid of two electronic height measurement gauges with sub-millimeter precision, mounted on the movable platform to ensure the gravel bed is leveled. The flow was uniform with a flow depth of 120 mm during the experiments. Mean flow velocity was estimated via two independent methods. Firstly, from the spatial average of the measured flow velocities across the channel. Secondly, from the mean flow discharge ( $Q$ ) of about  $8.5 \times 10^{-3} \text{ m}^3/\text{s}$ , calculated from the average measurements of electromagnetic flow meters attached to the inlet pipes via which water is circulated in the flume.

The test area was located 0.5 m from the downstream end of the vegetated region, where the flow became fully developed.

A series of acrylic support panels were placed above the riverbank, supported by steel framework bolted to the sidewall of the flume. A large number of acrylic rods (of diameter,  $D = 6$  mm) were placed on the support panel to model rigid emergent vegetation. The panels had a repeating pattern of drilled holes, which conveniently enabled placement of the rods at a certain location, having a distance  $x_i$  from each other (Figure 3a), up to a maximum distance of  $W_v = 0.32$  m. The bottom of each rod was cut at  $\theta = 17^\circ$ , to enable a perfect fit with the inclined bank surface. Six different vegetation densities were designed for this experiment (Figure 3b). Three of them were configured in linear arrangements, and the other three were configured in staggered arrangements (Figure 3b). With reference to previous studies, such as Nepf [27] and Tsujimoto et al. [28], the vegetation density of the array  $\lambda$  (per meter) can be defined as:

$$\lambda = \frac{\text{total projected rod area}}{\text{total volume}} = \frac{D}{x_i^2} \quad (1)$$

where  $x_i$  is the distance between each rod (Figure 3a), and  $D$  is the simulated vegetation element (rod) diameter. Table 1 summarizes the values of  $\lambda$  for each configuration. Kui et al. [22] conducted an experiment with 2 different densities of riparian vegetation, at 24 plants per  $\text{m}^2$  and 240 plants per  $\text{m}^2$ , which is within the range of number of plants per  $\text{m}^2$  in this study (Table 1). Both the vegetation density and the arrangement type of individual vegetation elements, are shown in Table 1. Figure 2b also indicates the relative location of the hydrodynamic measurements to the simulated vegetation elements (rods).

Measurements were taken using a side-looking ADV across the channel cross section, at a longitudinal distance of 4.2 m downstream from the location where the riverbank vegetation starts. As shown in Figure 2b, ten vertical velocity profiles were obtained—six of them located in the main channel and the rest of these located within the vegetated riverbank. The profiles in the main channel consisted of nine measurement points, and the profiles in the bank region comprised of six to nine measurement points depending on the maximum water depth at each location. Table 2 shows the coordinates of all measurement points, with the vertical distance referring to the distance from the solid boundary. At least 4-min records of the three-dimensional velocity vector were recorded with the ADV, at a frequency of 25 Hz for each measurement point. This recording frequency is sufficient to capture the essential features of the flow, as it is of relatively low turbulence ( $Re$  is about  $6 \times 10^3$  meaning that the turbulent fluctuations are not of high magnitude and turbulent mixing is not too vigorous, as happens in higher  $Re$  flows). More than 5000 raw data were obtained for each location recorded. During the experiments, the values of the ADV probe's signal to noise ratio (SNR) and correlation were also checked to ensure they met the minimum requirements suggested by the ADV manufacturer (15 dB and 70% respectively, [29]).

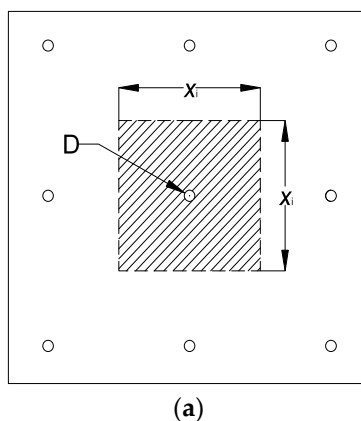
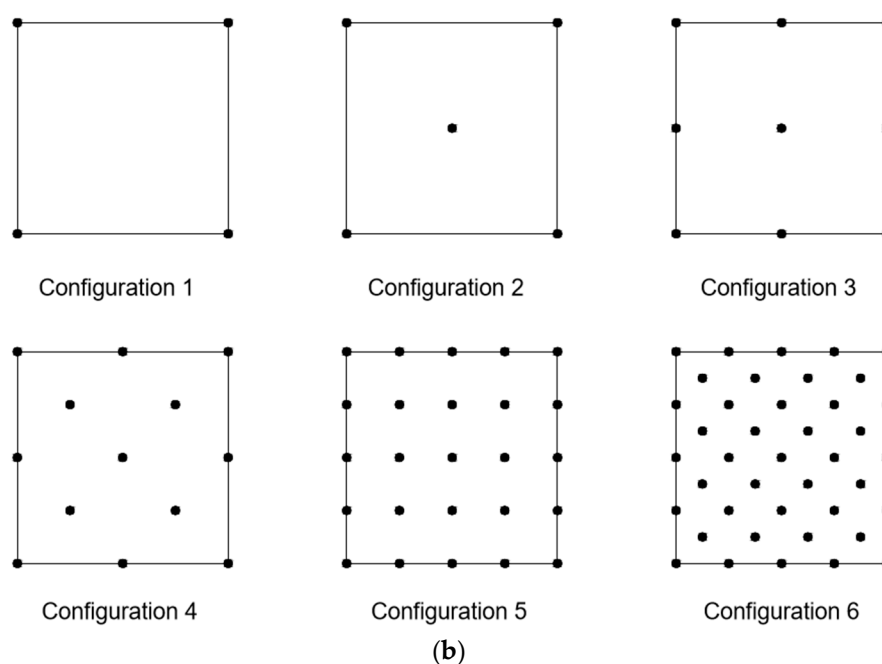


Figure 3. Cont.



**Figure 3.** (a) Definition sketch for the vegetation density, where the spacing of the elements for a configuration  $i$ , is denoted with  $x_i$ ; (b) Illustration of the configurations of simulated riverbank vegetation used in the experiments and the relative position of the flow measurements within the vegetated section. Increasing densities were achieved from one configuration to the next, by placing additional elements at the locations specified for this configuration (see corresponding shapes in the figure’s legend). Examples of elements’ spacing are shown for both linear ( $x_1$ ) and staggered ( $x_2$  and  $x_6$ ) configurations. With closed circles, the locations of the ADV measurement volume are indicated relative to the vegetation elements. Flow direction is along the  $x$ -axis.

**Table 1.** Vegetation density,  $\lambda$ , for each configuration.

Configuration (Density)	Rod Arrangement Type	$x_i$ [m]	$\lambda$ [ $\times 10^{-1} m^{-1}$ ]	Number of Plants per $m^2$
1 (low)	Linear	0.320	0.586	10
2 (low)	Staggered	0.226	1.172	20
3 (medium)	Linear	0.160	2.344	39
4 (medium)	Staggered	0.113	4.688	78
5 (high)	Linear	0.080	9.375	156
6 (high)	Staggered	0.057	18.75	308

**Table 2.** Specific coordinates denoting the location of flow velocity measurement volumes (with ADV) across the channel.  $y$  indicates the horizontal distance from the vertical side wall, and  $z$  indicates the vertical distance from the bed/bank surface.

$y$ [mm]	245	445	645	795	895	945	1010	1090	1170	1250
$z$ [mm]	100	100	100	100	100	100	91	68	41	21
	75	75	75	75	75	75	75	55	35	16
	55	55	55	55	55	55	55	35	20	12
	35	35	35	35	35	35	35	20	12	8
	20	20	20	20	20	20	20	12	8	5
	12	12	12	12	12	12	12	8	5	3
	8	8	8	8	8	8	8	5	3	*
	5	5	5	5	5	5	5	3	*	*
	3	3	3	3	3	3	3	*	*	*

Note: \* for the riverbank profiles, less data points were taken due to reduced flow depth.

Even though acoustic Doppler velocimeters (ADV) are widely used in both laboratory studies and field studies to obtain point measurements of the three-dimensional flow velocity, these measurements may at times record erroneous data, which may show as spikes in time series. These errors are caused by intrinsic Doppler noise, aliasing of the Doppler signal and perhaps due to the velocity gradient in the sampling volume [30,31]. Specific post-processing methods have been developed to remove such spikes in the raw velocity signal, aiming at the removal of any outliers and filtering of the records, such as the algorithms of Goring and Nikora [30] and Khorsandi et al. [32]. Herein, the raw velocity data collected by the ADV were post-processed using the method developed by Goring and Nikora [30]. Through their method, the high frequency part of the signal is enhanced by differentiation.

### 3. Results

#### 3.1. Streamwise Velocity

The mean velocity flow field can be represented either with the contour plots (Figure 4) showing the variation of flow hydrodynamics across the channel and the riverbank or with profile plots (Figure 5) enabling a more detailed comparison for a specific lateral location.

Observation of the mean streamwise velocity and its rate of change across the cross section of the channel can aid obtaining a better understanding for the strength of erosion processes at the riverbank in addition to the riverbed surface (Figure 4). From Figure 4, it is evident that the streamwise velocity in the vegetated riverbank dramatically decreases with increased riverbank vegetation density. This observation is in line with those reported in the literature. For example, the presence of vegetation on a sand bar likewise decreased the mean flow over the geomorphic feature but had the opposite effect across the rest of the main channel [10]. Herein, for  $\lambda = 1.88 \text{ m}^{-1}$ , the velocity in the riverbank is generally below 0.01 m/s, less than 6 times the average flow velocity in the main channel. The velocity in the riparian zone, particularly for the high vegetation densities, remains relatively constant across the water column following a rather suppressed logarithmic velocity profile, due to increased flow blockage (Figure 4).

The maximum flow velocity progressively increases with riparian vegetation density, also over a greater percentage of the cross-sectional area of the stream. The peak velocity for high vegetation density configurations ( $\lambda = 0.94$  and  $1.88 \text{ m}^{-1}$ ) reaches 0.07 m/s, reflecting the fact that a greater part of the flow rate is routed through the main channel compared to the case with lower riparian vegetation densities. The mean velocity at the boundary of the riparian zone, between the riverbank and the main channel (e.g., for  $y = 895 \text{ mm}$  and  $y = 945 \text{ mm}$ ) generally decreases with decreasing vegetation density. With increasing vegetation density at the riverbank, as the velocity at the main channel increases and the velocity at the riverbank reduces, a shear layer at the interface between the riverbank and main channel can be observed. The shear layer becomes more pronounced for high vegetation densities (see outlined sections for  $\lambda = 0.94$  and  $1.88 \text{ m}^{-1}$ , Figure 4).

The characteristic cases of mean velocity profiles at the centerline of the main channel ( $y = 445 \text{ mm}$ ) are shown in Figure 5. Specifically, the near bed surface and logarithmic region of the mean streamwise velocity profile are shown. It can be seen that near the top of the logarithmic region the flow velocity largely increases with vegetation density. So the smallest velocity is for the case of no vegetation at 0.050 m/s, increasing to about 0.052 m/s for low densities ( $\lambda = 0.06$  and  $0.12 \text{ m}^{-1}$ ), then to 0.055 m/s for medium densities ( $\lambda = 0.23$  and  $0.47 \text{ m}^{-1}$ ), up to 0.056 m/s for the high densities ( $\lambda = 0.94$  and  $1.88 \text{ m}^{-1}$ ).

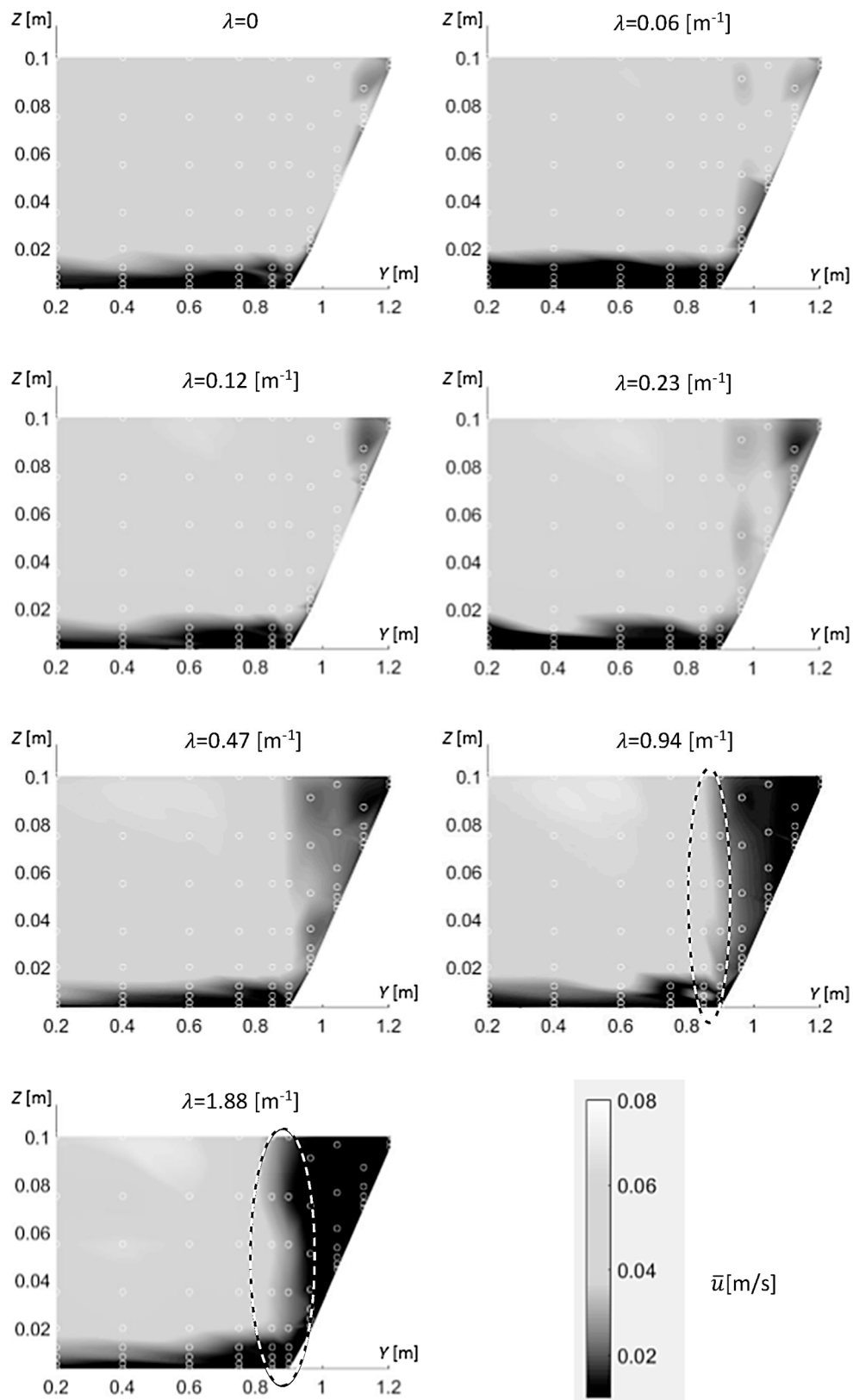


**Figure 4.** Contour plots of the mean streamwise velocity for the bare bank and each configuration (see Table 2) corresponding to increasing densities of the riverbank vegetation. The measurement locations are shown.  $z$  and  $y$  axes are not plotted to scale. Dashed circles indicate the region near the boundary of the main channel and the riverbank, where the shear layer is developing.



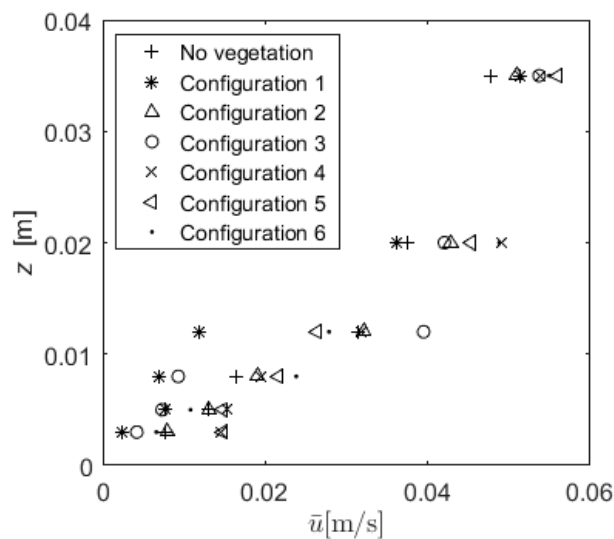


**Figure 5.** Streamwise mean velocity profiles at the centerline of the main channel ( $y = 445$  mm) for the bare streambank and various riparian density configurations (1–6; see Table 2 for details).

Near-bed flow velocities remain low due to the resistance of the solid boundary, regardless of the density of riparian vegetation. However, as the vegetation density increases and more of the flow rate is routed through the main channel, the flow velocity gradient, and subsequently Reynolds stresses, at the main channel will also increase. This means that even though the shear stresses are reduced at the riverbank, they increase at the main channel, along with the potential for eroding and deepening the main channel further. To substantiate this qualitative description, the bed-shear stresses at the main channel are estimated using the velocity profiles under the assumption of the log Law of the Wall. It needs to be emphasized that the mean streamwise velocity profiles inside the vegetated riverbank are not following the logarithmic profile, thus the log-Law approximation does not apply. This can be observed for all cases shown in Figure 4, where the streamwise flow velocity at the riverbank does not exhibit a consistent change across the flow depth. This is in accordance to the observations of past studies, reporting non-logarithmic shapes for the streamwise velocity profiles past vegetation patches [11,33].

### 3.2. Bed-Shear Stresses

The streamwise velocity profiles at the main channel generally follow the logarithmic law for turbulent flows over a solid boundary:

$$\bar{u} = AU_f \ln\left(\frac{30(z' - z_1)}{k_s}\right) \quad (2)$$

where  $A$  is a constant ( $A = 2.5$ ),  $U_f$  is the frictional velocity,  $z' - z_1$  is the distance between the measurement location and the theoretical bed surface level,  $k_s$  is Nikuradse's equivalent sand grain roughness [34]. The average value of  $k_s$ , representative of the average roughness across the main channel, reduces from 23 mm to 12 mm, for low to high vegetation density. This value is about 6 to 11.5 times the value of  $D_{50}$  at the surface of the sand bed for this study and is in agreement with past findings in the literature. For example, Cheng [35] reported that  $k_s$  equals 5 to 12.9 times of the median diameter of bed material, while Madsen [36] reported that  $k_s$  equals to 15 times of the median diameter of sand bed.

Under the assumption of a logarithmic profile at the turbulent boundary layer region, the representative special average of the bed-shear stresses at the centerline of the main channel are estimated to be  $\tau = 0.007$  Pa for the cases of no and low riverbank vegetation ( $\lambda = 0$  to  $0.12 \text{ m}^{-1}$ ). This is seen to

increase with riverbank vegetation, following an almost linear trend up to the value of  $\tau = 0.013$  Pa for the case of dense riverbank vegetation ( $\lambda = 1.9 \text{ m}^{-1}$ ). This is a significant increase of up to 86% comparing the cases of no and dense vegetation. This corresponds to a value for Shields' shear stress of  $\tau_* = \frac{U_f^2}{g(\rho_s - \rho)D_{50}} = O(10^{-4})$ , which is much below the critical value (which is  $O(10^{-2})$ ) for the transport of sediment.

### 3.3. Turbulence Intensity

Even though bed-shear stresses have been used as the standard criterion for assessing riverbed and riverbank erosion, recent criteria put strong emphasis on the role of flow turbulence and coherent flow structures [7,24,25]. Likewise, contemporary research on riparian vegetation hydrodynamics and their potential implications for sediment transport suggest that there is little certainty that shear stresses are the sole criterion to accurately describe these interactions and propose criteria based on turbulent fluctuations [37].

Turbulence intensity is an important flow hydrodynamics diagnostic measure, denoting the magnitude and variability of turbulent fluctuations, which may be important in understanding the potential for sediment transport. Herein, the turbulence intensity in the streamwise and lateral flow direction is analyzed. It is defined as the ratio of the standard deviation of the streamwise velocity over the bulk mean flow component:

$$\frac{\sqrt{u_i'^2}}{U} = \frac{\sqrt{\frac{1}{n} \sum_{i=1}^n (u_i - \bar{u})^2}}{U} \quad (3)$$

$$\frac{\sqrt{v_i'^2}}{V} = \frac{\sqrt{\frac{1}{n} \sum_{i=1}^n (v_i - \bar{v})^2}}{V} \quad (4)$$

where  $U$  and  $V$  are the spatially and temporally averaged streamwise and lateral flow velocity respectively, which here are kept constant to the value of  $U = 0.045$  m/s and  $V = 0.003$  m/s;  $u_i$  and  $v_i$  are the instantaneous (recorded) streamwise and lateral flow velocity respectively, and  $n$  is the number of measured velocity records over the time window of estimation.

As Figure 6 shows, turbulence intensity in the streamwise direction ranges from 0.05 to 0.24 across the water column for the various configurations. The shape of the turbulence intensity profiles at the main channel is typical of open channel flows (e.g., for  $y = 445$  mm, Figure 6), showing an increase to its peak value at about 10–12 mm above the solid boundary and then rapidly decreasing with increasing flow depth. This is physically justified by the fact that most of the turbulence production happens near the solid boundary. This shape can also be seen at the boundary of the main channel and the vegetated riverbank (e.g., for  $y = 895$  mm and  $y = 945$  mm), although the shape is less standard.

For the higher vegetation densities at the riverbank, turbulence intensity reduces and obtains the smallest values for the denser configuration (e.g.,  $\lambda = 0.94$  and  $1.88 \text{ [m}^{-1}]$ , see Figures 6 and 7), due to the blockage to the flow. However, it is evident that turbulence levels at the main channel and near the riverbank slightly increase with riparian vegetation density (Figures 6 and 7), possibly due to increased turbulence mixing induced by it. The comparison of the peak values of turbulence intensities at the main channel (for  $y = 445$  mm) and the vicinity of the toe of the riverbank (for  $y = 945$  mm), for each configuration, can be seen in Table 3. Similarly, for the rest of the locations at the main channel (for  $y = 895$  and  $945$  mm), the lowest density configurations ( $\lambda = 0.06$  and  $0.12 \text{ m}^{-1}$ ) correspond to greater turbulence levels (ranging from 0.20 to 0.22).

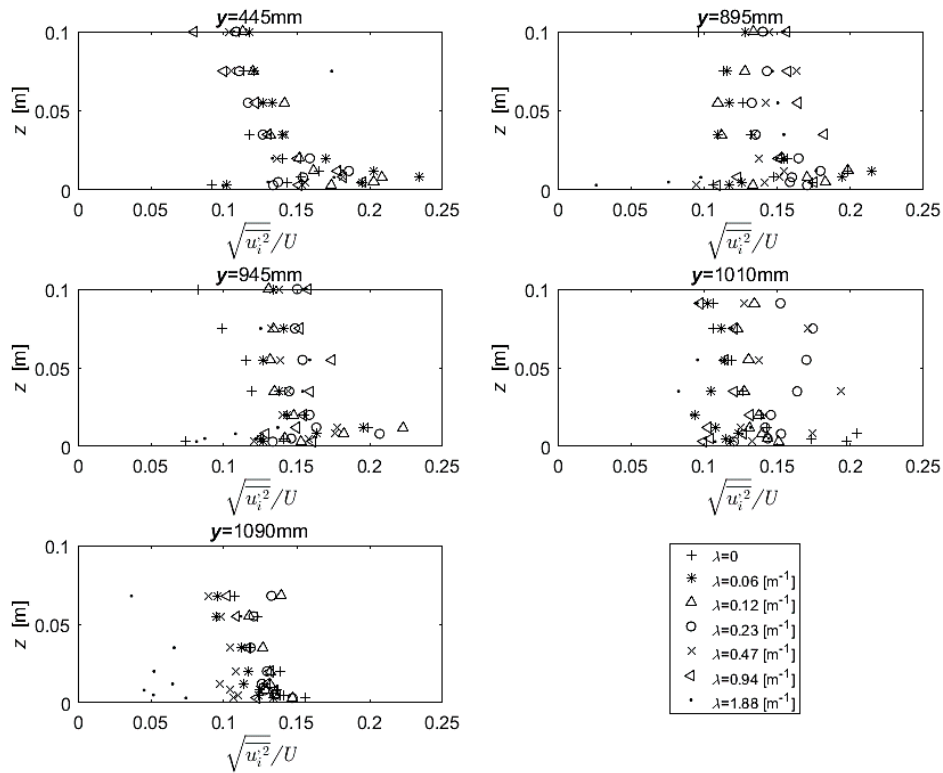


**Figure 6.** Plots of streamwise turbulence intensity profiles for characteristic transverse locations: at the main channel (for  $y = 445$  mm); at the region between the main channel and the riverbank (for  $y = 895$  and  $945$  mm); and within the sloping bank (for  $y > 1000$  mm).

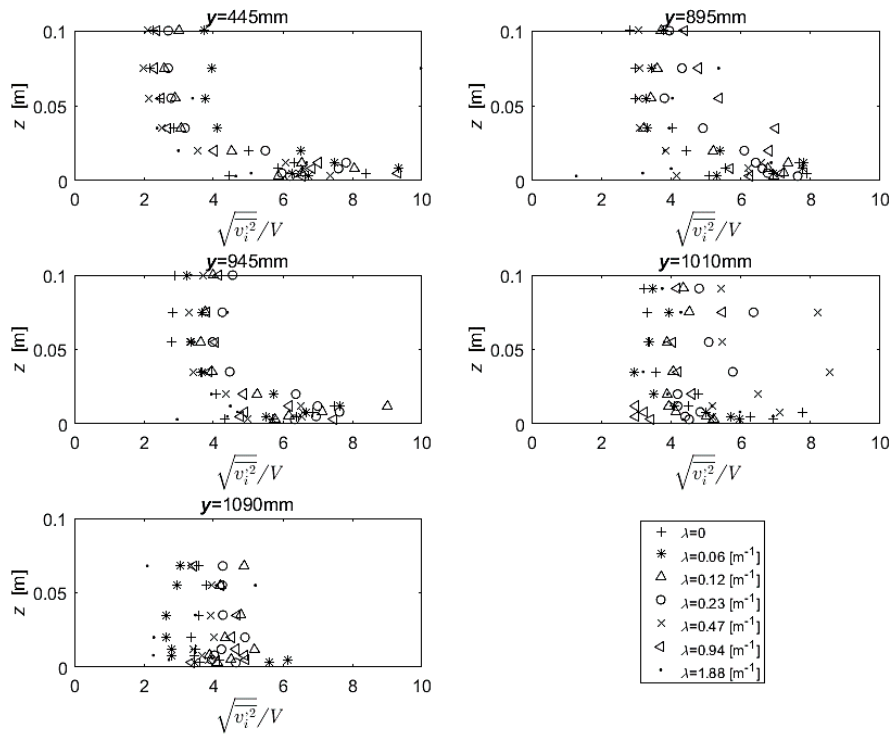


**Figure 7.** Plots of lateral turbulence intensity profiles for characteristic transverse locations: at the main channel (for  $y = 445$  mm); at the region between the main channel and the riverbank (for  $y = 895$  and  $945$  mm); and within the sloping bank (for  $y > 1000$  mm).

**Table 3.** The maximum observed streamwise values at the main channel (profile  $y = 445$  mm) and the toe of the riverbank (profile  $y = 945$  mm), and the percentage increase compared to the case of bare riverbank (no riparian vegetation).

$\lambda$ [ $\text{m}^{-1}$ ]		0	0.06	0.12	0.23	0.47	0.94	1.88
$y = 445$ mm	$\frac{\sqrt{u_i'^2}}{U_{max}}$	0.16	0.23	0.21	0.18	0.18	0.19	0.18
	Change compared to no vegetation	0%	42%	27%	12%	15%	17%	9%
$y = 945$ mm	$\frac{\sqrt{u_i'^2}}{U_{max}}$	0.20	0.20	0.22	0.21	0.18	0.15	0.14
	Change compared to no vegetation	0%	−2%	12%	4%	−11%	−25%	−31%

It is useful to quantify these changes by comparing the maximum streamwise turbulent intensity near the bed surface for the case of configurations with increasing vegetation density to the case of no bare riverbank (no vegetation). There appears to be a consistent trend for the ratio of streamwise turbulent intensities for each configuration to the bare riverbank, as shown in Figure 8. Specifically, this is shown to be largely reducing near the riverbank (profile  $y = 945$  mm) by about 36% from the case of low vegetation densities ( $\lambda = 0.06$  and  $0.12 \text{ m}^{-1}$ ) to the case of high densities ( $\lambda = 0.94$  and  $1.88 \text{ m}^{-1}$ ). The same reduction is observed for the same ratio at the main channel centerline, but at a smaller magnitude of 15% (Figure 8).

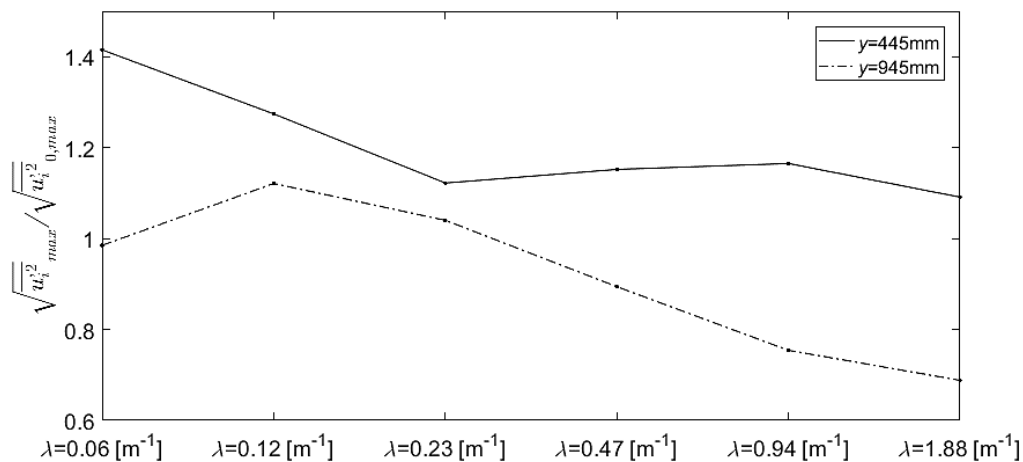


**Figure 8.** Ratios of the highest streamwise turbulent intensity values of each different vegetation density  $\frac{\sqrt{u_i'^2}}{U_{max}}$  in the main channel to the highest turbulent intensity value for no riverbank vegetation  $\frac{\sqrt{u_i'^2}}{U_{0,max}}$ . Results for two different locations are shown: at the centerline of the main channel ( $y = 445$  mm) and at the vicinity of the toe of the riverbank ( $y = 945$  mm).

These results demonstrate that within a densely vegetated riverbank, the flow slows down significantly, additionally resulting in a reduction of the strength of the macroscale flow structures advected along the riverbank and their impingement length, as has been also demonstrated by [37]. This is also consistent with the observations of reduced shear stress with increasing riverbank vegetation, overall leading to reduced riverbank destabilization potential for the higher vegetation densities (e.g.,  $\lambda = 0.94$  to  $1.9 \text{ m}^{-1}$ ). However, for the lower vegetation densities, the effect of individual vegetation elements on flow hydrodynamics is observed with increased turbulence levels due to the shedding of eddies past them (e.g., for  $\lambda \approx 0$  to  $0.12 \text{ m}^{-1}$ ). These effects are stronger at the riverbank toe region. In a natural setting, this would increase the potential for destabilizing the riverbank. Thus

even though riparian vegetation is generally thought to generally stabilize soil with its root system [38], for low vegetation densities it may instead have adverse effects, leading to local scour (particularly near the riverbank's toe region) and overall promoting bank erosion.

## 4. Discussion

### 4.1. Interactions between Riparian Vegetation and Hydrogeomorphology

Insight into how different riverbank vegetation densities influence flow hydrodynamics has practical implications for applied river management, including managing vegetation to convey flood flows and the design and adaptive management of river restoration schemes [39–41]. With respect to the latter, there is increased recognition that interactions and feedback between vegetation, water flow and sediment dynamics, control channel and floodplain form and dynamics [1,42]. If restoration schemes are to be successful in enhancing river process and form, scheme designs must account for how riparian and emergent aquatic vegetation will influence hydrogeomorphology. Gurnell [1] present a conceptual model of vegetation-hydrogeomorphological interactions that divides a river corridor into five zones depending upon their relation with magnitude and frequency of inundation, fine sediment deposition, and sediment erosion and deposition. The model provides a basis for framing the effect of riverbank vegetation densities on flow hydrodynamics and morphology.

With respect to the experimental results reported in this paper, two zones of the model are of greatest relevance since they are in the critical zone of vegetation-hydrogeomorphology interaction. Zone one of the river corridor, the river channel, which is permanently inundated; it is the zone with deepest water, highest velocities, and greatest bed-shear stresses across all flows. Sediment transport rates are thus at their greatest within this zone, resulting in a habitat that is hostile to vegetation growth and survival. Zone two, the immediate riverbank, is frequently inundated by high flows and is also characterized by sediment transport but riparian and emergent aquatic plants can survive in this zone, depending upon their tolerance to fluvial disturbance in the form of inundation, scour and burial [43,44]. The results presented in this research suggest that bed-shear stresses at the main channel (zone one) can have an up to twofold increase (comparing the bare riverbank and one with dense vegetation of  $\lambda \sim 2 \text{ m}^{-1}$ ). This means that while it is beneficial to protect the riverbank (zone 2) with vegetation, the maximum riverbank density should be also controlled, so as to avoid reducing the flow through it to a level that can lead to deepening of the streambed. So there seems to be a compromise between low and high vegetation densities and offering a better understanding of the processes involved towards finding a “sweet spot” or optimal riverbank density for protecting both riverbed and riverbanks, and this has been the focus of this research. However, interactions between vegetation, flow, sediment transport and morphology in zones one and two of a river restoration scheme are likely to be longitudinally and laterally more complex, than what is shown in this controlled study, due to the irregular and patchy nature of vegetation colonization and survival, response to floods, and temporal shifts in hydrogeomorphological processes.

### 4.2. Case Studies and Best Practices: Examples from the UK

River restoration by channel realignment is currently being trialed across a number of upland rivers in the United Kingdom to enhance natural river processes and improve morphological diversity along previously straightened reaches. These realignment schemes are typically morphologically dynamic in their first year, as they adjust from their imposed design during the first sequence of high flow events that they are exposed to. This short-term morphological adjustment occurs at the same time as riverbank vegetation establishes, either through planting or natural colonization, and starts to influence flow, and sediment erosion and deposition.

Investigation of early vegetation-hydrogeomorphology feedbacks on a realignment scheme on the lowland River Cole, United Kingdom, indicates that feedbacks between naturally colonizing vegetation, hydro- and sediment-dynamics on the riverbank are significant within one year of realignment [45].

Figure 9 shows a sequence of photos that have been taken to record the evolution of the upland Whit Beck river restoration scheme, Cumbria. The true left bank (left of the images) is adjacent to a wooded area and, at decadal scales, trees are likely to develop along this river bank and exert influence on channel form. Rapid vegetation colonization, subsequent scour and burial during flooding in December 2015 [46], followed by further vegetation colonization in autumn 2016 and spring 2017 is evident on the right bank and bar. Vegetation colonization of the bar concentrates flow into a narrower and deeper channel, and may thus increase erosion on the outer bank. Such feedbacks have also been observed at point bars of sandy experimental rivers [10]. The arrangement of plastic tree sapling guards can be seen on both banks; whilst these saplings do not currently exert a significant influence on channel hydrodynamics, as the trees establish they are likely to.

The research proposed herein and the experiment results reported in this paper could be used to provide broad guidance on the spatial layout and density of planting, as well as for maintaining riverbank vegetation once fully established. For example, the arrangement of plastic tree sapling guards can be seen on both banks (e.g., Figure 9c); whilst these saplings do not on their own exert a significant influence on channel hydrodynamics, as the riparian vegetation establishes further, they are likely to. In the first case, the arrangement of tree sapling and planted vegetation was relatively sparse, with a representative density closer matching a scaled version of the second and third experimental configurations (Figure 8c,d, respectively). Even though the vegetation density has grown denser at specific locations, the high flow has eroded part of the riverbank with lower vegetation density. According to the results and hydrodynamic metrics presented herein, sparse riverbank vegetation is not able to significantly protect the bank slope from erosion during high flows (Figure 8e,f). Thus it is noted that planting riparian vegetation, which will at a sufficient density by the time of high flood events, may help to better protect against erosion at the riverbank.



**Figure 9.** Six fixed-point photos that were acquired at a fixed point on the Whit Beck River restoration scheme, Cumbria, United Kingdom, during a 21-month period. Images look in a downstream direction. (a) Newly realigned river, showing initial riverbank vegetation. (b) Bar formation on true right, following first storm event. (c) Colonization of riverbank grasses and tree planting. (d) Colonization of bar with grasses. (e) High flows and midchannel bar development, following the December 2015 Cumbrian floods [46]. (f) Further establishment of vegetation on true left; unvegetated bar on true right after reworking. (g–i) Vegetation establishment and growth on true right bar.

For the example of a tributary at the Water of Girvan, in Scotland, presented earlier (Figure 1), the use of revegetation techniques, such as planting native vegetation species and placing willow fagots, offers a sustainable method that engineers and consultants use widely to prevent riverbank erosion. Figure 1b shows that a sandbar has formed about five months after the installation of willow fagot and shootings of native species planted at the earlier eroded part of the riverbank (see also [47]). This effectively reduces the flow and hydrodynamic forcing through the affected region, allowing for fine bed material and sand to deposit behind it, allowing for the riverbank to re-establish. This is the same region as the interface of the main channel and riverbank, which is shown to typically exhibit higher shear stresses, posing a risk for initiating local scour and subsequently full scale bank erosion. This method allows for the establishment of a flow regime similar to the densely vegetated riverbank in our experiments ( $\lambda = 0.94$  and  $1.88 \text{ m}^{-1}$ ), with reduced hydrodynamic stresses (by more than 50% on average), at the same region (e.g., for  $y > 1000 \text{ mm}$ ). This method is more effective to planting shootings alone, as young plants may not have established at a sufficiently high density or have developed a strong root system to sustain the hydrodynamic action of turbulent flows [48,49].

#### 4.3. Implications for Riverbank Stability

Overall, it can be seen from the velocity and turbulence intensity profiles (Figures 5 and 6) that hydrodynamic stresses within the riverbank region evidently decrease with increasing riparian vegetation. In this study, the riverbank is designed as nonerodible bank (thus the effect of the root system is not evaluated) and the vegetation elements are rigid (not flexible) cylinders without canopy. Flexibility of the vegetation elements is perhaps most important for higher flows or smaller riverbank densities, potentially leading to overestimating the effect on hydrodynamics compared to naturally flexible vegetation. However, this effect is expected to be counterbalanced by the presence of leafy canopy that interacts with the flow as vegetation becomes submerged. These are features that can be modelled in a future flume studies.

In this series of experiments, the obtained results are demonstrative of the potential of using riverbank vegetation in reducing the hydraulic erosional capacity of high flows at the riverbank, compared to the bare bank or low riparian vegetation densities. As the research herein emphasizes, for increased vegetation densities, increases riverbank blockage and routing of the flow towards the main channel can erode and deepen the main channel. Monitoring the riverbank vegetation to avoid erosion at the riverbank or main channel respectively, by combining the observations from this study and river corridor restoration frameworks [50] or via embedding in appropriate deterministic or stochastic modelling approaches to ecosystem management [51], has the potential to comprehensively address this challenge.

Chen et al. [52] linked the erosional capacity of the flow to the enhanced bed-shear stresses near the exposed part of instream vegetation. In this study it is found that both bed-shear stress estimates and turbulence intensity results offer consistent trends for the increasing potential of destabilization of the main channel and toe of the riverbank, for high and low vegetation densities respectively. However, as this study has demonstrated, bed-shear stresses cannot be estimated with certainty assuming logarithmic velocity profiles, nor other ways of estimation offer consistent results [11]. This makes it of even greater utility and urgency to identify relevant criteria, which can be used and associated to riverbank stability. Further analysis using recently suggested event-based criteria for sediment transport, which appropriately accounts for the scales of coherent turbulent flow structures [53,54] and relevant modelling tools [24,25,55], would be also relevant to pursue in future studies. Such efforts should focus on investigating the potential of such criteria to better characterize the erosive capacity of flow turbulence on riverbanks, and find practical applications on vegetation flow hydrodynamics, engineering ecohydraulics and fluvial geomorphology.

## 5. Conclusions

A series of appropriately designed flume experiments with increasing riverbank vegetation density were conducted to study vegetation-hydrodynamic interactions with implications on hydro-geomorphologic feedbacks. In particular, hydrodynamic measurements were taken along the cross section of an open channel flow with a simulated nonerodible vegetated riverbank with different densities or riparian vegetation. The range of densities, sparse and dense, assessed in this study are representative of a range of natural systems, as suggested by the literature [56–58]. Turbulent flow measurements and hydrodynamic analysis comprising of mean velocity and turbulent intensity profiles and bed-shear stresses, offer consistent trends.

At the main channel, comparing the cases of no vegetation to the cases with dense vegetation ( $\lambda = 1.9 \text{ m}^{-1}$ ), bed-shear stresses can significantly increase (up to about two times) and streamwise turbulent intensities can also increase by about 40%. This is due to a relative “flow blockage” effect of the densely vegetated riverbanks leading to the increased routing of the bulk of the flow to the main channel, potentially leading to destabilization of the main channel.

At the riverbank toe region, turbulence intensity reduces up to 40% for the cases of low-to-high vegetation densities ( $\lambda \approx 0$  to  $1.9 \text{ m}^{-1}$ ), implying that the potential for erosion decreases with increasing vegetation density. This is due to an increased “flow agitation” effect from the individual vegetation elements when located in a sparse arrangement. This mechanism is largely silenced by the “flow blockage” effect as the vegetation density increases.

Even though hydrodynamic measurements are obtained near and within the riverbank, existing criteria such as traditionally estimated bed-shear stresses, cannot assess comprehensively and with certainty the risk of destabilization. It is suggested that these will be comprehensively evaluated in a future study, potentially including estimation of flow impulses and energetic flow events due to coherent turbulent flow structures.

As the two mechanisms presented above can destabilize the main channel bed or toe of the riverbank for very high or very low vegetation densities, respectively, careful consideration needs to be practiced so as to ensure that adverse effects are avoided. For practical case studies, it is suggested to undertake a thorough hydrodynamic monitoring campaign at the sections of interest (e.g., adjacent to critical infrastructure) of a rehabilitated river and aim to control riverbank vegetation density by following the framework and analysis similar to what is presented here, towards identifying the most appropriate range of vegetation densities (not too low, nor too high) weakening the effects of the above mechanisms (also largely dependent on the expected flow rates and bed surface topography, varying per case). Such recommendations can help amend existing best practices for river management and environmentally sustainable restoration, preventing riverbank destabilization.

**Acknowledgments:** This work was partially supported by the Royal Society (Research Grant RG2015 R1 68793/1) and the Royal Society of Edinburgh research grants.

**Author Contributions:** M.V. and D.L. conceived and designed the experiments; D.L. performed the experiments and analyzed the data; M.V., R.W. and D.L. contributed to the discussion; D.L. wrote the paper.

**Conflicts of Interest:** The authors declare no conflicts of interest.

## References

1. Gurnell, A.M. Plants as river system engineers. *Earth Surf. Process. Landf.* **2014**, *39*, 4–25. [[CrossRef](#)]
2. Scottish Environment Protection Agency (SEPA). Reducing river bank erosion. In *A Best Practice Guide for Farmers and Other Land Managers*; Scottish Environment Protection Agency: Stirling, UK, 2016.
3. Scottish Environment Protection Agency (SEPA). Engineering in the water environment good practice guide. In *Bank Protection: Rivers and Lochs*, 1st ed.; Scottish Environment Protection Agency: Stirling, UK, 2008.
4. Iowa Department of Natural Resources. *How to Control Streambank Erosion*; Natural Resources Conservation Service, U.S. Department of Agriculture, Ed.; Iowa Department of Natural Resources: Des Moines, IA, USA, 2006.



5. Zong, L.; Nepf, H. Flow and deposition in and around a finite patch of vegetation. *Geomorphology* **2010**, *116*, 363–372. [[CrossRef](#)]
6. Valyrakis, M.; Kitsikoudis, V.; Yagci, O.; Kirca, V.S.O.; Koursari, E. Experimental investigation of the modification of the flow field, past emergent aquatic vegetation elements. In Proceedings of the 36th IAHR World Congress, The Hague, The Netherlands, 28 June–3 July 2015.
7. Yagci, O.; Celik, M.F.; Kitsikoudis, V.; Ozgur Kirca, V.S.; Hodoglu, C.; Valyrakis, M.; Duran, Z.; Kaya, S. Scour patterns around isolated vegetation elements. *Adv. Water Resour.* **2016**, *97*, 251–265. [[CrossRef](#)]
8. Yager, E.M.; Schmeeckle, M.W. The influence of vegetation on turbulence and bed load transport. *J. Geophys. Res. Earth Surf.* **2013**, *118*, 1585–1601. [[CrossRef](#)]
9. Wilson, C.A.M.E.; Stoesser, T.; Bates, P.D.; Pinzen, A.B. Open channel flow through different forms of submerged flexible vegetation. *J. Hydraul. Eng.* **2003**, *129*, 847–853. [[CrossRef](#)]
10. Rominger, J.T.; Lightbody, A.F.; Nepf, H.M. Effects of added vegetation on sand bar stability and stream hydrodynamics. *J. Hydraul. Eng.* **2010**, *136*, 994–1002. [[CrossRef](#)]
11. Hopkinson, L.; Wynn, T. Vegetation impacts on near bank flow. *Ecohydrology* **2009**, *2*, 404–418. [[CrossRef](#)]
12. Czarnomski, N.M.; Tullios, D.D.; Thomas, R.E.; Simon, A. Effects of vegetation canopy density and bank angle on near-bank patterns of turbulence and reynolds stresses. *J. Hydraul. Eng.* **2012**, *138*, 974–978. [[CrossRef](#)]
13. Afzalimehr, H.; Najfabadi, E.F.; Singh, V.P. Effect of vegetation on banks on distributions of velocity and reynolds stress under accelerating flow. *J. Hydraul. Eng.* **2010**, *15*, 708–713. [[CrossRef](#)]
14. Darby, S.E.; Thorne, C.R.; Member, A. Predicting stage-discharge curves in channels with bank vegetation. *J. Hydraul. Eng.* **1996**, *122*, 583–586. [[CrossRef](#)]
15. Thorne, C.R.; Hey, R.D.; Newson, M.D. *Applied Fluvial Geomorphology for River Engineering and Management*; John Wiley & Sons: Chichester, UK, 1997.
16. Couper, P.R.; Maddock, I.P. Subaerial river bank erosion processes and their interaction with other bank erosion mechanisms on the river arrow, Warwickshire, UK. *Earth Surf. Process. Landf.* **2001**, *26*, 631–646. [[CrossRef](#)]
17. Lawler, D.M.; Grove, J.R.; Couperthwaite, J.S.; Leeks, G.J.L. Downstream change in river bank erosion rates in the swale-ouse system, northern england. *Hydrol. Process.* **1999**, *13*, 977–992. [[CrossRef](#)]
18. Carson, M.A.; Kirkby, M.J. *Hillslope Form and Process*; Cambridge University Press: London, UK, 1972.
19. Hubble, T.C.T.; Docker, B.B.; Rutherford, I.D. The role of riparian trees in maintaining riverbank stability: A review of australian experience and practice. *Ecol. Eng.* **2010**, *36*, 292–304. [[CrossRef](#)]
20. Erskine, W.; Keene, A.; Bush, R.; Cheetham, M.; Chalmers, A. Influence of riparian vegetation on channel widening and subsequent contraction on a sand-bed stream since european settlement: Widden brook, Australia. *Geomorphology* **2012**, *147–148*, 102–114. [[CrossRef](#)]
21. Chen, S.-C.; Chan, H.-C.; Li, Y.-H. Observations on flow and local scour around submerged flexible vegetation. *Adv. Water Resour.* **2012**, *43*, 28–37. [[CrossRef](#)]
22. Kui, L.; Stella, J.C.; Lightbody, A.; Wilcox, A.C. Ecogeomorphic feedbacks and flood loss of riparian tree seedlings in meandering channel experiments. *Water Resour. Res.* **2014**, *50*, 9366–9384. [[CrossRef](#)]
23. Schmeeckle, M.W. Numerical simulation of turbulence and sediment transport of medium sand. *J. Geophys. Res. Earth Surf.* **2014**, *119*, 1240–1262. [[CrossRef](#)]
24. Valyrakis, M.; Diplas, P.; Dancey, C.L. Prediction of coarse particle movement with adaptive neuro-fuzzy inference systems. *Hydrol. Process.* **2011**, *25*, 3513–3524. [[CrossRef](#)]
25. Valyrakis, M.; Diplas, P.; Dancey, C.L. Entrainment of coarse grains in turbulent flows: An extreme value theory approach. *Water Resour. Res.* **2011**, *47*, W09512. [[CrossRef](#)]
26. Da Silva, Y.J.A.B.; Cantalice, J.R.B.; Singh, V.P.; Cruz, C.M.C.A.; Silva Souza, W.L.D. Sediment transport under the presence and absence of emergent vegetation in a natural alluvial channel from brazil. *Int. J. Sediment Res.* **2016**, *31*, 360–367. [[CrossRef](#)]
27. Nepf, H.M. Drag, turbulence, and diffusion in flow through emergent vegetation. *Water Resour. Res.* **1999**, *35*, 479–489. [[CrossRef](#)]
28. Tsujimoto, T.; Shimizu, Y.; Kitamura, T.; Okada, T. Turbulent open-channel flow over bed covered by rigid vegetation. *J. Hydrosoci. Hydraul. Eng.* **1992**, *10*, 13–25.
29. Vectrino Velocimeter User Guide. Available online: <http://www.nortek-as.com/en/support/manuals> (accessed on 19 September 2017).

30. Goring, D.G.; Nikora, V.I. Despiking acoustic Doppler velocimeter data. *J. Hydraul. Eng.* **2002**, *128*, 117–126. [[CrossRef](#)]
31. Lohrmann, A.; Cabrera, R.; Karus, N.C. Acoustic-Doppler velocimeter (ADV) for laboratory use. In *Hydraulic Measurements and Experimentation, Proceedings Sponsored by Hydraulics Division/ASCE, Buffalo, NY, USA, 1–5 August 1994*; ASCE: Reston, VA, USA, 1994; pp. 351–365.
32. Khorsandi, B.; Mydlarski, L.; Gaskin, S. Noise in turbulence measurements using acoustic doppler velocimetry. *J. Hydraul. Eng.* **2012**, *138*, 829–838. [[CrossRef](#)]
33. Yang, J.Q.; Chung, H.; Nepf, H.M. The onset of sediment transport in vegetated channels predicted by turbulent kinetic energy. *Geophys. Res. Lett.* **2016**. [[CrossRef](#)]
34. Guo, J.; Julien, P.Y. Shear stress in smooth rectangular open-channel flows. *J. Hydraul. Eng.* **2005**, *131*, 30–37. [[CrossRef](#)]
35. Cheng, N.-S. Representative grain size and equivalent roughness height of a sediment bed. *J. Hydraul. Eng.* **2016**, *142*, 06015016. [[CrossRef](#)]
36. Camenen, B.; Larson, M.; Bayram, A. Equivalent roughness height for plane bed under oscillatory flow. *Estuar. Coast. Shelf Sci.* **2009**, *81*, 409–422. [[CrossRef](#)]
37. Nepf, H.M. Hydrodynamics of vegetated channels. *J. Hydraul. Eng.* **2012**, *50*, 262–279. [[CrossRef](#)]
38. Edmaier, K.; Burlando, P.; Perona, P. Mechanisms of vegetation uprooting by flow in alluvial non-cohesive sediment. *Hydrol. Earth Syst. Sci.* **2011**, *15*, 1615–1627. [[CrossRef](#)]
39. Beechie, T.J.; Sear, D.A.; Olden, J.D.; Pess, G.R.; Buffington, J.M.; Moir, H.; Roni, P.; Pollock, M.M. Process-based principles for restoring river ecosystems. *BioScience* **2010**, *60*, 209–222. [[CrossRef](#)]
40. Wohl, E.; Lane, S.N.; Wilcox, A.C. The science and practice of river restoration. *Water Resour. Res.* **2015**, *51*, 5974–5997. [[CrossRef](#)]
41. Curran, J.C.; Hession, W.C. Vegetative impacts on hydraulics and sediment processes across the fluvial system. *J. Hydrol.* **2013**, *505*, 364–376. [[CrossRef](#)]
42. Osterkamp, W.R.; Hupp, C.R.; Stoffel, M. The interactions between vegetation and erosion: New directions for research at the interface of ecology and geomorphology. *Earth Surf. Process. Landf.* **2012**, *37*, 23–36. [[CrossRef](#)]
43. Steiger, J.; Tabacchi, E.; Dufour, S.; Corenblit, D.; Peiry, J.L. Hydrogeomorphic processes affecting riparian habitat within alluvial channel–floodplain river systems: A review for the temperate zone. *River Res. Appl.* **2005**, *21*, 719–737. [[CrossRef](#)]
44. McShane, R.R.; Auerbach, D.A.; Friedman, J.M.; Auble, G.T.; Shafroth, P.B.; Merigliano, M.F.; Scott, M.L.; Poff, N.L. Distribution of invasive and native riparian woody plants across the western USA in relation to climate, river flow, floodplain geometry and patterns of introduction. *Ecography* **2015**, *38*, 1254–1265. [[CrossRef](#)]
45. Gurnell, A.M.; Boitsidis, A.J.; Thompson, K.; Clifford, N.J. Seed bank, seed dispersal and vegetation cover: Colonization along a newly-created river channel. *J. Veg. Sci.* **2006**, *17*, 665–674. [[CrossRef](#)]
46. Burt, S.; McCarthy, M.; Kendon, M.; Hannaford, J. Cumbrian floods, 5/6 December 2015. *Weather* **2016**, *71*, 36–37. [[CrossRef](#)]
47. Pasquale, N.; Perona, P.; Francis, R.; Burlando, P. Effects of streamflow variability on the vertical root density distribution of willow cutting experiments. *Ecol. Eng.* **2012**, *40*, 167–172. [[CrossRef](#)]
48. Polvi, L.E.; Wohl, E.; Merritt, D.M. Modeling the functional influence of vegetation type on streambank cohesion. *Earth Surf. Process. Landf.* **2014**, *39*, 1245–1258. [[CrossRef](#)]
49. Tron, S.; Perona, P.; Gorla, L.; Schwarz, M.; Laio, F.; Ridolfi, L. The signature of randomness in riparian plant root distributions. *Geophys. Res. Lett.* **2015**, *42*, 7098–7106. [[CrossRef](#)]
50. Pasquale, N.; Perona, P.; Schneider, P.; Shrestha, J.; Wombacher, A.; Burlando, P. Modern comprehensive approach to monitor the morphodynamic evolution of a restored river corridor. *Hydrol. Earth Syst. Sci.* **2011**, *15*, 1197–1212. [[CrossRef](#)]
51. Perona, P.; Camporeale, C.; Perucca, E.; Savina, M.; Molnar, P.; Burlando, P.; Ridolfi, L. Modelling river and riparian vegetation interactions and related importance for sustainable ecosystem management. *Aquat. Sci.* **2009**, *71*, 266–278. [[CrossRef](#)]
52. Chen, L.; Acharya, K.; Stone, M.C. Using a mechanical approach to quantify flow resistance by submerged, flexible vegetation—A revisit of kouwens’ approach. *Adv. Water Resour.* **2014**, *73*, 198–202. [[CrossRef](#)]

53. Diplas, P.; Dancey, C.L.; Celik, A.O.; Valyrakis, M.; Greer, K.; Akar, T. The role of impulse on the initiation of particle movement under turbulent flow conditions. *Science* **2008**, *322*, 717–720. [[CrossRef](#)] [[PubMed](#)]
54. Valyrakis, M.; Diplas, P.; Dancey, C.L.; Greer, K.; Celik, A.O. Role of instantaneous force magnitude and duration on particle entrainment. *J. Geophys. Res. Earth Surf.* **2010**, *115*, F02006. [[CrossRef](#)]
55. Perona, P.; Molnar, P.; Savina, M.; Burlando, P. An observation-based stochastic model for sediment and vegetation dynamics in the floodplain of an alpine braided river. *Water Resour. Res.* **2009**, *45*, W09418. [[CrossRef](#)]
56. Poggi, D.; Porporato, A.; Ridolfi, L.; Albertson, J.D.; Katul, G.G. The effect of vegetation density on canopy sub-layer turbulence. *Bound.-Layer Meteorol.* **2004**, *111*, 565–587. [[CrossRef](#)]
57. Rominger, J.T.; Nepf, H.M. Flow adjustment and interior flow associated with a rectangular porous obstruction. *J. Fluid Mech.* **2011**, *680*, 636–659. [[CrossRef](#)]
58. Belcher, S.E.; Jerram, N.; Hunt, J.C.R. Adjustment of a turbulent boundary layer to a canopy of roughness elements. *J. Fluid Mech.* **2003**, *488*, 369–398. [[CrossRef](#)]



© 2017 by the authors. Licensee MDPI, Basel, Switzerland. This article is an open access article distributed under the terms and conditions of the Creative Commons Attribution (CC BY) license (<http://creativecommons.org/licenses/by/4.0/>).